On the Processes Leading to Carotenemia-Elicited Changes in the Spectral Responses and Chromatic Attributes of Human Skin

Gladimir V. G. Baranoski[1]

Abstract—The presence of large concentrations of carotenoids within human skin, normally referred to as carotenemia, has been associated with a myriad of photobiological phenomena with a direct impact on the population's health. Despite the diverse body of biomedical research in this area, there are still key aspects that remain elusive with respect to the cutaneous accumulation of these compounds and their effects on skin and light interactions. Accordingly, the current understanding about the spectral responses and chromatic attributes of affected skin specimens, notably those characterized by high levels of pigmentation, is hindered by empirical information paucity. In this paper, we address these interconnected processes and their implications for the assessment of individuals' carotenemic status. To achieve that, we conducted controlled *in silico* experiments supported by measured data. We also discuss different strategies for the cost-effective monitoring of carotenoids' accumulation in skin sites more exposed to ultraviolet light and characterized by distinct levels of pigmentation.

Index Terms—Carotenoids, carotenemia, photoprotection, skin, pigmentation, reflectance, color, *in silico* experiments.

I. Introduction

Carotenoids are lipophilic pigments that occur naturally in plant and participate in the photosynthesis process [1]. Although animals and humans are unable to synthesize these compounds, they can obtain them through their diet or supplements. Humans absorb approximately one-third of the ingested carotenoids [2]. Among the most common carotenoids found in human tissues is β-carotene, which is a provitamin A, a precursor of immunomodulatory vitamin A [3], [4], [5].

Carotenemia (or carotenodermia [4]) is a condition associated with high concentrations of carotenoids within the cutaneous tissues and the blood stream [2], [6]. It is known to affect the spectral responses and chromatic attributes of human skin, notably in individuals characterized by relatively low levels of skin pigmentation [7]. In theses cases, the relatively low presence of melanin (Fig. 1(a)) and hemoglobin (Fig. 1(b)), the major absorbers of visible light within the cutaneous tissues, results in more light being absorbed by carotenoids like β-carotene (Fig. 1(c)). This, in turn, elicits a yellowish skin tint [1], [8] while also leading to a reduction of skin reflectance in the visible spectral domain [7].

Besides contributing to the skin color, carotenoids also play important protective roles such as the absorption of

ultraviolet (UV) radiation [9], [7]. Although the UV protection offered by carotenoids is considered to be weaker than that offered by sunscreens, it is known to be effective over a longer period of time and, for practical purposes, to cover nearly the entire skin [4]. Moreover, their anti-oxidant properties mitigate the harmful consequences of elevated amounts of reactive oxygen species (ROS) [4], [10]. Once the ROS concentration within a tissue exceeds a critical value, cell and cell components can be irreversably impaired. This may lead to significant tissue damage and even cancer [4], [5], [9], [11]. From a cosmetic standpoint, carotenoids also positively affect skin morphophysiological aspects like elasticity and moisture [4], [5].

As prompted by a large ingestion of carotenoids, carotenemia is considered a benign condition [2], [6], [12], [13]. However, it is important to note that a number of serious medical conditions, such as hypothyroidism, diabetes mellitus, hepatic disorders and renal diseases, may lead to the onset of carotenemia despite not being caused by the excessive ingestion of carotenoids [2], [8], [14], [15], [16].

Given the biomedical ramifications of carotenemia outlined above, it becomes relevant to further the current knowledge about the intrinsic mechanisms of this condition and their effects on the spectral responses and chromatic attributes of human skin. A deeper understanding about these aspects can pave the way for the development of more cost-effective procedures aimed at enhancing the systemic protection offered by carotenoids and improving the screening of pathologies that may give rise to carotenemia.

It has been postulated that there are two main pathways for the accumulation of carotenoids within the cutaneous tissues. The first, and arguably the most investigated, corresponds to the diffusion from adipose tissue, blood and lymph nodes [4], [5]. It has been observed that plasma levels of β-carotene are correlated with their respective concentration in the cutaneous tissue [4], [9]. The second corresponds to the secretion via sweat glands and/or sebaceous glands onto the skin surface, and their subsequent penetration into the cutaneous tissues [5]. As a consequence of these pathways, carotenoids can be found in the stratum corneum, epidermis (normally divided into stratum granulosum, spinosum and basale) and dermis (composed of papillary and reticular dermis and their respective networks of blood vessels) [5], [7], [17]. This can result in distinct carotenoids' accumulation patterns within the various cutaneous tissues.

To the best of our knowledge, the effects of these accumulation patterns on the spectral responses and the chromatic attributes of human skin have not been comprehensively

examined to date. In the research presented in this paper, our main objectives are to systematically investigate these interconnected processes and to expedite the translation of the obtained insights to practical use.

Among the reasons for the current scarcity of scientific information and quantitative data in this area, one can highlight the difficulties to conduct controlled experiments to assess these effects. Often carotenemia studies are based on the use of skin samples obtained through autopsy or biopsy procedures [17], [9], [5], [4]. These samples are likely to have their optical properties altered under *in vitro* conditions. In the case of biopsies, they can pose risks to a subject's health due to their invasive nature. Another approach involves the use of spectrophotometric measurements [7], [9], [10]. Although such a noninvasive approach has proven to be useful for several biomedical applications [5], [9], it depends on the subjects' ingestion of large amount of carotenoids whose absorption may be difficult to control since it may vary from one subject to the next. This makes the precise quantification and distribution of carotenoids within each skin layer more difficult to be achieved during spectrophotometric measurements.

In order to overcome the aforementioned technical constraints, we employed an *in silico* approach supported by measured data. It enabled us to conduct a detailed examination of the impact that different carotenoids' accumulation patterns can have on skin spectral responses and chromatic attributes, and to obtain reliable and repeatable insights about these interconnected biophysical processes. Without lack of generality, we elected to consider β-carotene as the representative carotenoid in our *in silico* experiments. This choice was motivated by its prominent presence in related investigations in this area [1], [9], [7], [17], being not only one the most abundant carotenoids, but also one the mostly widely studied [4], [18]. These aspects also facilitated the gathering of qualitative information and measured data relevant for this research.

In our investigation, we paid special attention to aspects often overlooked in related works in this area. For instance, most carotenemia studies (*e.g.*, [5], [6], [7], [9], [14], [19], [20]) involve primarily lightly-pigmented or moderately-pigmented specimens. Generally speaking, relatively little is known about its effects on the spectral responses and chromatic attributes of individuals with a high level of constitutive (genetically determined) pigmentation [7], [10]. Due to the masking effects of the melanins, major light absorbers in the UV and visible spectral domains, the carotenemia effects on these individuals are often assessed in skin sites characterized by hypopigmentation such as those found in the palm of the hands [7], [19]. However, from a photoprotection perspective, nonhypopigmented skin sites, such as those normally found in the face, dorsum of the hands, arms and legs, are more likely to be exposed to UV radiation. Accordingly, for this investigation, we considered three skin specimens representative of nonhypopigmented sites with markedly distinct levels of constitutive pigmentation (lightly, moderately and darkly pigmented).
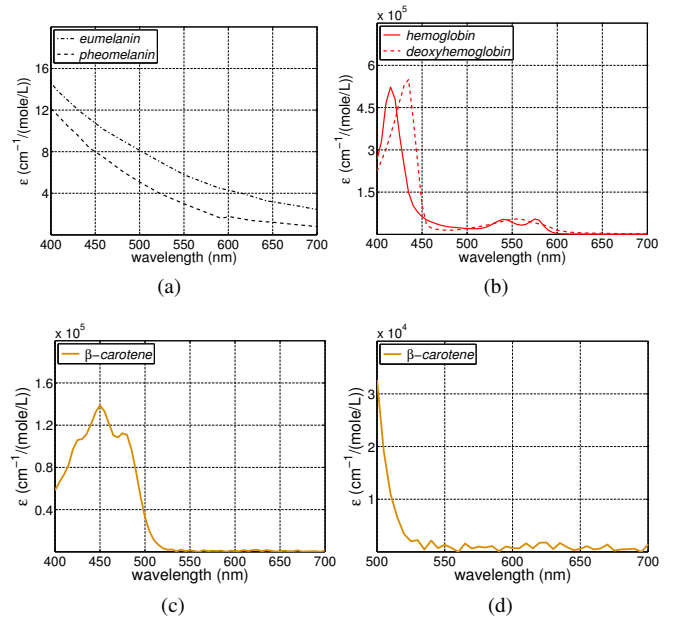

Fig. 1: Absorption spectra of key pigments considered in this work. (a) Melanins [21]. (b) Functional hemoglobins [22]. (c) β-carotene's [23]. (d) Zoom-in of the β-carotene's absorption spectrum in the 500-700 nm interval.

II. Materials and Methods

The lightly pigmented, moderately pigmented and darkly pigmented skin specimens employed in this investigation are henceforth referred to as LP, MP and DP, respectively. The parameter values used in their characterization are provided in Tables I and II. We note that the selection of these values was based on biophysically valid ranges provided in the literature, whose sources are listed elsewhere [24], [25] for conciseness, and used measured reflectance curves acquired from real specimens [26], [27] as references. This strategy enabled us to obtain well-grounded baselines for our controlled *in silico* experiments. More specifically, the measured reflectance curves for the LP and MP specimens were provided by Vrhel *et al.* [26], while the measured curve for the DP specimen was provided by Jacquez *et al.* [27].

To conduct our *in silico* experiments, we employed the first-principles model of light and skin interactions known as HyLIoS (*Hyperspectral Light Impingement on Skin*) [24]. More precisely, we used it to compute directional-hemispherical reflectance curves for the specimens. Within the HyLIoS' ray-optics algorithmic formulation, a ray interacting with the tissues of a skin specimen can be associated with any wavelength (λ) within a spectral domain of interest (the visible region, 400-700 nm, in this investigation).

It is worth mentioning that the HyLIoS' predictive capabilities have been extensively evaluated through quantitative and qualitative comparisons of its outcomes with actual measured data [24]. Since then, this model has been effectively employed in several related biomedical investigations (*e.g.*, [25], [28], [29], [30]). For reproducibility purposes, we have made HyLIoS accessible for online use [31]. Also, all supporting

TABLE I: Parameters employed in characterization of the selected lightly pigmented (LP), moderately pigmented (MP) and darkly pigmented (DP) skin specimens.

Parameter	LP	MP	DP
Ratio of Skin Surface Folds	0.10	0.25	0.45
SC Thickness (cm)	0.0010	0.0010	0.0002
SG Thickness (cm)	0.0011	0.0033	0.0009
SS Thickness (cm)	0.0011	0.0033	0.0009
SB Thickness (cm)	0.0011	0.0033	0.0009
PD Thickness (cm)	0.04	0.01	0.03
RD Thickness (cm)	0.1	0.1	0.2
SG Melanosome Cont. (%)	0.75	0.0	7.5
SS Melanosome Cont. (%)	0.75	0.22	7.5
SB Melanosome Cont. (%)	0.75	3.75	7.5
SG Colloidal Melanin Cont. (%)	3.75	1.25	12.5
SS Colloidal Melanin Cont. (%)	3.75	1.25	12.5
SB Colloidal Melanin Cont. (%)	3.75	1.25	12.5
Melanosome Dim. ($\mu m \times \mu m$)	0.36×0.14	0.41×0.17	0.69×0.28
Eumelanin Conc. (g/L)	50.0	50.0	50.0
Pheomelanin Conc. (g/L)	4.0	2.0	1.0
PD Blood Cont. (%)	0.18	1.2	2.5
RD Blood Cont. (%)	0.18	0.8	2.5
Oxygenated Hb Frac. (%)	85.0	90.0	85.0
Functional Hb Conc. (g/L)	140.0	130.0	147.0
Radius of PD Scatterers (nm)	100.0	80.0	100.0

Notes: The acronyms SC, SG, SS, SB, PD and RD refer to the stratum corneum, stratum granulosum, stratum spinosum, stratum basale, papillary dermis and reticular dermis tissues, respectively. The acronym Hb refers to hemoglobin.

TABLE II: Parameters kept fixed during the simulations.

Parameter	Value
SC Melanosome Cont. (%)	0.0
SG Colloidal Melanin Cont. (%)	0.0
Melanosome Complex Diam./Axis	2.0
Melanin Refractive Index	1.7
Methemoglobin Conc. in Blood (g/L)	1.5
Carboxyhemoglobin Conc. in Blood (g/L)	1.5
Sulfhemoglobin Conc. in Blood (g/L)	0.0
Bilirubin Conc. in Blood (g/L)	0.003
SC Water Cont. (%)	35.0
Epidermis Water Cont. (%)	90.0
PD Water Cont. (%)	65.0
RD Water Cont. (%)	75.0
SC Lipid Cont. (%)	10.0
Epidermis Lipid Cont. (%)	1.0
PD Lipid Cont. (%)	5.0
RD Lipid Cont. (%)	5.0
SC Keratin Cont. (%)	55.0
SC Urocanic Acid Density (mol/L)	0.01
Skin DNA Density (g/L)	0.185
Melanin Refractive Index	1.7
SC Refractive Index	1.55
Epidermis Refractive Index	1.4
PD Refractive Index	1.39
RD Refractive Index	1.41
PD Scatterers Refractive Index	1.5
PD Fraction Occupied by Scatterers (%)	22.0

Note: The acronyms SC, SG, SS, SB, PD and RD refer to the stratum corneum, stratum granulosum, stratum spinosum, stratum basale, papillary dermis and reticular dermis tissues, respectively.

TABLE III: Normal and anomalous (mild and accentuated) concentrations (in g/L) of β-carotene considered in this investigation. For the mild and accentuated cases, we account for the anomalous presence of β-carotene in the *epidermal* tissues only, *dermal* tissues only (D), and in *all* tissues (A).

Tissue	Normal	Mild			Accentuated		
		E	D	A	E	D	A
SC	2.1E-4	0.5E-2	2.1E-4	0.5E-2	1.5E-2	2.1E-4	1.5E-2
SG	2.1E-4	0.5E-2	2.1E-4	0.5E-2	1.5E-2	2.1E-4	1.5E-2
SS	2.1E-4	0.5E-2	2.1E-4	0.5E-2	1.5E-2	2.1E-4	1.5E-2
SB	2.1E-4	0.5E-2	2.1E-4	0.5E-2	1.5E-2	2.1E-4	1.5E-2
PD	7.5E-5	7.5E-5	0.5E-2	0.5E-2	7.5E-5	1.5E-2	1.5E-2
RD	7.5E-5	7.5E-5	0.5E-2	0.5E-2	7.5E-5	1.5E-2	1.5E-2
Blood	7.5E-5	7.5E-5	0.5E-2	0.5E-2	7.5E-5	1.5E-2	1.5E-2

Note: The acronyms SC, SG, SS, SB, PD and RD refer to the stratum corneum, stratum granulosum, stratum spinosum, stratum basale, papillary dermis and reticular dermis tissues, respectively.

datasets (*e.g.,* the extinction coefficients depicted in Fig. 1) employed in our *in silico* experiments are openly available in a dedicated data repository [32].

In our baseline experiments, we computed the reflectance curves for the examined specimens in their normal state using concentrations of β-carotene reported in the literature [17] for cutaneous tissues not affected by carotenemia. The selected values for these concentrations are presented in Table III. For comparison purposes, the computation of the baseline reflectance curves was carried out considering the same angles of incidence (θ_i) used in the acquisition of the measured reflectance curves employed as references for our investigation. More precisely, the modeled curves for the LP and MP specimens were obtained considering θ_i equal to $45°$ [26], while the modeled curve for the DP specimen was obtained considering θ_i equal to $16.75°$ [27].

As it can be observed in Fig. 2, the modeled curves presented a close agreement with their measured counterparts. Moreover, the root mean square errors calculated for the modeled curves with respect to the measured curves were notably low (0.0115, 0.0054, 0.0076 for the LP, MP and DP specimens, respectively). These aspects further indicated a high degree of fidelity of the predictions provided by the employed *in silico* experimental framework, and reinforced the plausibility of the characterization datasets selected for the LP, MP and DP specimens.

We then proceeded to conduct the controlled *in silico* experiments to assess the effects of the presence of anomalous β-carotene concentrations in the cutaneous tissues. For consistency, all modeled curves computed during these experiments, including the control curves associated with normal β-carotene concentrations, were obtained considering the same angle of incidence, namely θ_i equal to $0°$.

In these experiments, we considered different groups of cutaneous tissues associated with the main pathways for the accumulation of β-carotene in human skin. We denominated these groups as *epidermal* (comprising only the stratum corneum, granulosum, spinosum and basale), *dermal* (comprising only the papillary and reticular dermis as well as their blood vessels networks) and *all* (comprising all the aforementioned tissues). The anomalous β-carotene concentrations employed in these experiments were classified as mild and accentuated (carotenemic states). Their respective values are depicted in Table III, and they were also based on values reported in the literature [2], [33].

Subsequently, we employed the modeled reflectance curves to obtain the skin chromatic attributes associated
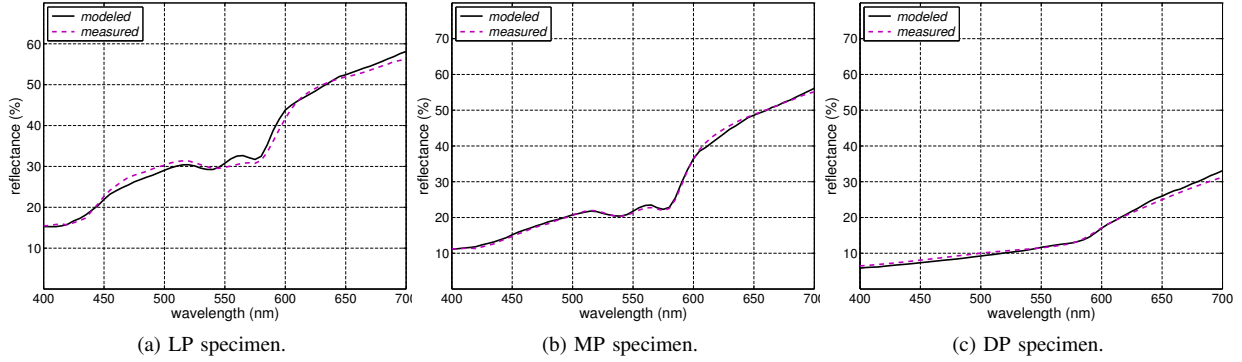
Fig. 2: Comparison between modeled and measured spectral reflectance curves for the selected specimens. The measured curves for the LP and MP specimens were obtained by Vrhel *et al.* [26] considering θ_i equal to $45°$, while the measured curve for the DP specimen was obtained by Jaquez *et al.* [27] considering θ_i equal to $16.75°$. The modeled curves were computed considering the specimens' characterizations datasets present in Tables I and II, and the normal amounts of β-carotene presented in Table III.

with the distinct carotenemic states under investigation. More specifically, these attributes were computed through the convolution of a selected illuminant's relative spectral power distribution, the modeled reflectance data and the broad spectral response of the human photoreceptors [34]. This last step was carried out using a standard CIEXYZ to sRGB color system conversion procedure [35] and considering the standard CIE D65 (ambient light) illuminant [34]. The resulting colors were then used to generate skin swatches through the application of a grayscale texture.

Besides the visual inspection of the skin swatches, we also used a device-independent CIE-based metric to compare the resulting modeled skin chromatic attributes. More precisely, we calculated the CIELAB differences between the colors (before their achromatic relative brightness modulation by the grayscale texture) associated with pairs of swatches using the following formula [36]:

$$\Delta E_{ab}^* = \sqrt{(d_L{}^2 + d_a{}^2 + d_b{}^2)}, \tag{1}$$

where d_L, d_a and d_b denote the differences $L_1^* - L_2^*$, $a_1^* - a_2^*$ and $b_1^* - b_2^*$, respectively, in which L^* (representing darkness/lightness), a^* (representing the balance between reds and greens) and b^* (representing the balance between yellows and blues) correspond the CIELAB color space dimensions. These are calculated for the modeled chromatic attributes (colors) associated with the compared swatches (indicated by the subscripts 1 and 2). Again, we performed these calculations using standard formulas employed in colorimetry [37] and considering the CIE D65 illuminant [34].

III. RESULTS AND DISCUSSION

As shown in Fig. 3, the mild carotenemic state led to reflectance decreases in the 500-525 nm and 600-700 nm intervals for all considered carotenoids' distributions (*epidermal*, *dermal* and *all*) within the tissues belonging to the LP and MP specimens. For the DP specimen, only a minor reflectance decrease was observed in the 600-700 nm interval for all tissues. This can be explained by

the melanins' and hemoglobins' masking effects, which are stronger for this specimen characterized by a larger presence of these pigments. However, their absorption spectra is lower in the 600-700 nm region (Figs. 1(a) and (b)), while the absorption spectrum of β-carotene in this interval, albeit relative lower then that associated with the 400-600 nm interval, is not negligible (Figs. 1(c) and (d)). Overall, the reflectance variations were more noticeable for the *dermal* distributions than for the *epidermal* distributions in the 400-525 nm and 600-700 nm intervals for the LP and MP specimens. For all three specimens, the reflectance variations were negligible in the 525-600 nm interval for all considered carotenoids' distributions. For the DP specimen, the reflectance variations associated with the *epidermal* distribution were negligible across the entire visible region, and only minor variations associated with the *dermal* distribution were observed in 600-700 nm interval.

Similar trends were verified for the accentuated carotenemic state as indicated in Fig 4. However, more prominent reflectance decreases were observed for the LP and MP specimens with respect to the *epidermal* distribution. For the LP specimen, it was also observed a reflectance decrease, associated with the *dermal* distribution, in the 525-600 nm interval. For the MP specimen, the reflectance curves associated with the *epidermal* and *dermal* distributions were closer in the 400-525 nm interval. For the DP specimen, the reflectance decrease associated with the *dermal* distribution became more pronounced in the 600-700 nm interval.

In Fig. 5, we present the swatches obtained using the reflectance curves provided in Fig. 3 for the mild carotenemic state. The depicted skin appearances show that, for the LP specimen, the chromatic transitions to a yellow tint were noticeable for the *dermal* distribution, but not for the *epidermal* distribution. For the MP specimen, the transition to a yellow tint was also noticeable for the *dermal* distribution, albeit less evident than that observed for the LP specimen, and no noticeable chromatic transition was observed for the *epidermal distribution*. For the DP specimen, no chromatic
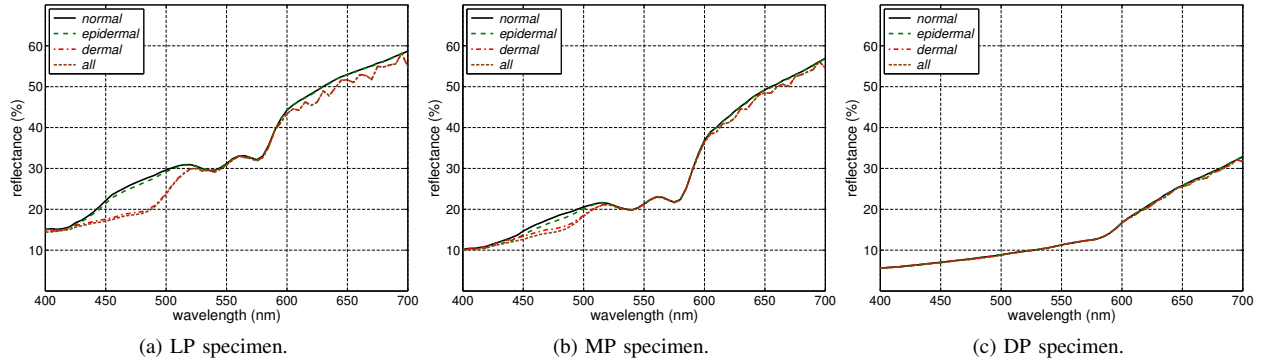
| (a) LP specimen. | (b) MP specimen. | (c) DP specimen. |

Fig. 3: Effects of a mild carotenemia (0.005 g/L of β-carotene in the affected tissues as indicated in Table III) on the spectral reflectance of the selected specimens. Each depicted curve is associated with a group of affected tissues: *epidermal* (stratum corneum, granulosum, spinosum and basale), *dermal* (papillary dermis, reticular dermis and their blood supplies) and *all* (*epidermal* and *dermal*) tissues. For comparison purposes, the control curves obtained considering *normal* concentrations of β-carotene (Table III) are also provided. All curves were obtained considering θ_i equal to $0°$.

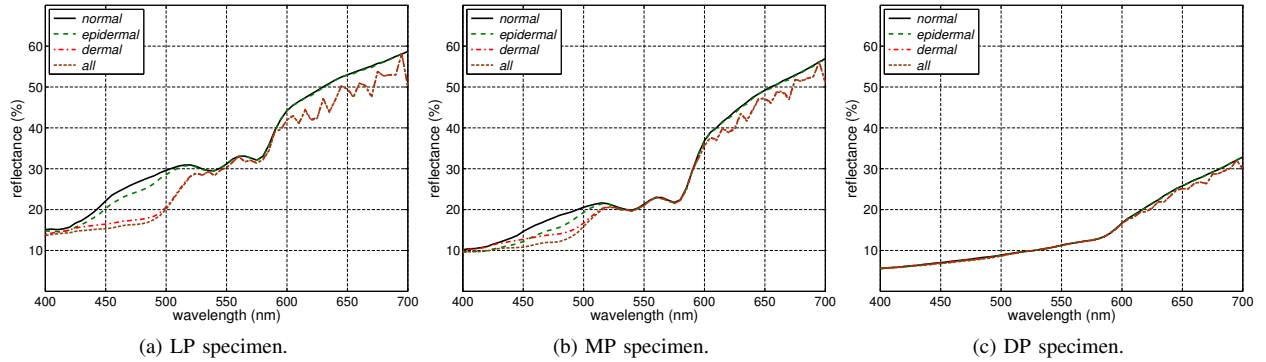| (a) LP specimen. | (b) MP specimen. | (c) DP specimen. |

Fig. 4: Effects of an accentuated carotenemia (0.015 g/L of β-carotene in the affected tissues as indicated in Table III) on the spectral reflectance of the selected specimens. Each depicted curve is associated with a group of affected tissues: *epidermal* (stratum corneum, granulosum, spinosum and basale), *dermal* (papillary dermis, reticular dermis and their blood supplies) and *all* (*epidermal* and *dermal*) tissues. For comparison purposes, the control curves obtained considering *normal* amounts of β-carotene (Table III) are also provided. All curves were obtained considering θ_i equal to $0°$.

transitions were verified. These observations are supported by the CIELab differences depicted in Table IV for the mild carotenemic state. We note that differences below 2.3, which corresponds to an empirically determined human perceptibility threshold [36], [38], indicate that the associated chromatic transitions cannot be detected by an average human observer.

In Fig. 6, we present the swatches obtained using the reflectance curves provided in Fig. 4 for the accentuated carotenemic state. For this state, the depicted skin appearances show that the transitions to a yellow tint were stronger than those verified for the mild carotenemic state. For the LP specimen, the transitions were noticeable for the *epidermal* and *dermal* distributions, and stronger for the latter. For the MP specimen, the transitions were also noticeable for *epidermal* and *dermal* distribution, but stronger for the former. For the DP specimen, no transitions were noticeable. Again, these visual observations were also supported by the CIELab differences depicted in Table IV for the accentuated carotenemic state.

Alaluf *et al.* [7] and Perrett *et al.* [19] suggested that the CIELab b^* dimension could be used to assess skin carotenoid status and the degree of skin "yellowness" elicited by carotenemia, respectively. However, both studies were based on measurements conducted primarily on lightly and moderately pigmented individuals. The authors of both studies indicated the need of extending their investigations to darkly pigmented specimens.

Accordingly, we calculated the b^* values associated with the chromatic attributes of the LP, MP, and DP specimens in their normal and carotenemic states. As it can be observed in the rows of Table V, the anomalous presence of β-carotene in *all* tissues led to an increase in the b^* values obtained for the LP and MP specimens considering both carotenemic states. However, for specimen DP, such an increase was verified only for the accentuated carotenemic state. Also, for all three specimens, we did not observe a direct correlation between b^* and the anomalous presence of β-carotene either in the *epidermal* or in the *dermal* tissues. Hence, the use of b^* as a marker for different carotenoids' distributions within the cutaneous tissues is not unfailing. Moreover, as it can also be observed in the columns of Table V, b^* values did not correlate with the specimens' level of pigmentation.

Fig. 5: Swatches depicting the appearance of the light pigmented (LP), moderately pigmented (MP) and darkly pigment (DP) specimens in their corresponding mild carotenemic states associated with the reflectance curves presented in Fig. 3. These were obtained considering the normal and anomalous presence of β-carotene in the *epidermal* tissues, *dermal* tissues and in *all* tissues, respectively.

Fig. 6: Swatches depicting the appearance of the light pigmented (LP), moderately pigmented (MP) and darkly pigment (DP) specimens in their corresponding accentuated carotenemic states associated with the reflectance curves presented in Fig. 4. These were obtained considering the normal and anomalous presence of β-carotene in the *epidermal* tissues, *dermal* tissues and in *all* tissues, respectively.

TABLE IV: CIELAB ΔE_{ab}^* differences computed for the chromatic attributes of the LP, MP and DP specimens in the mild (Fig. 5) and accentuated (Fig. 6) carotenemic states (in comparison with their normal chromatic attributes) considering the anomalous presence of β-carotene in the *epidermal* tissues, *dermal* tissues and in *all* tissues.

	Mild			Accentuated		
	Epidermal	Dermal	All	Epidermal	Dermal	All
LP	**1.21**	7.75	8.86	3.19	8.93	11.22
MP	**1.96**	2.88	4.77	5.68	4.11	8.74
DP	**0.0**	**0.0**	**0.0**	**0.55**	**0.92**	**1.13**

Note: Values below the perceptibility threshold (2.3) [36], [38] are presented in boldface.

Clearly, high levels of constitutive pigmentation pose additional challenges to the investigation of different carotenoids' accumulation patterns. Usually, noninvasive spectrophotometric procedures proposed for the assessment of skin carotenoids status are focused on radiometric responses obtained in the spectral region where the β-carotene absorption spectrum is higher (Fig. 1 (c)). However, the absorption spectra of the melanins (Fig. 1 (a)) and hemoglobins (Fig. 1 (b)) are high in this region as well, which creates measurement difficulties, notably for darkly pigmented specimens.

To mitigate the melanins and hemoglobins' masking effects, we propose the use of spectral responses obtained in the 600-700 nm interval. Although the absorption spectrum of β-carotene is low in this interval, it is not negligible (Fig. 1 (d)). Based on the reflectance ($\rho(\lambda)$) curves presented in Figs. 3 and 4, two possible tests could be executed to determine the predominant occurrence of *epidermal* or *dermal* carotenoids' accumulations in target specimens:

TABLE V: CIELAB color space b^* dimension calculated for the chromatic attributes of the LP, MP, and DP specimens in their normal and carotenemic states (mild and accentuated) considering the anomalous presence of β-carotene in the *epidermal* tissues, *dermal* tissues and in *all* tissues.

		Mild			Accentuated		
	Normal	Epidermal	Dermal	All	Epidermal	Dermal	All
LP	24.2	25.4	31.7	32.8	27.3	32.5	34.8
MP	25.6	27.5	28.3	30.3	31.3	29.4	34.1
DP	21.5	21.5	21.5	21.5	22.0	21.1	22.4

1) If $\rho(670) < abs(\rho(645) - \rho(695))$ then the accumulation is predominantly *dermal*. Otherwise, it is predominantly *epidermal*.

2) If $\rho(670) < \rho(695)$ then the accumulation is predominantly *dermal*. Otherwise, it is predominantly *epidermal*.

Although both tests provide the expected results for the carotenemic states associated with the reflectance curves presented in Figs. 3 and 4, test #1 may be more appropriate for general use. We note that test #2 requires only two spectral samples, but it employs a resolution of 5 nm. Although the test #2 requires three spectral samples, it employs a resolution of 25 nm, *i.e.*, more space between the samples. Thus, it is less susceptible to measurement uncertainties or spectral shifts in the skin pigments' absorption spectra.

IV. CONCLUSION

Considering the connection of the *dermal* accumulation of carotenoids with the primary pathway for the distribution of these compounds within human skin, notably involving their transport through the dermal blood network, this ac-

cumulation pattern may have a more direct influence on an individual's health than the *epidermal* pattern. Our findings indicate that it may also have a larger impact on the carotenemic specimens' spectral responses and chromatic attributes.

Based on the outcomes of our *in silico* experiments, we note that the use of chromatic attributes, or color parameters derived from them, in the assessment of different carotenoids' accumulation patterns becomes unreliable for specimens characterized by high pigmentation levels. On the other hand, it may be improved by using the specimens' spectral responses in the red end of the visible spectrum.

Clearly, as with any *in silico* investigation, our findings are still subject to confirmation through *in situ* experiments. Nonetheless, we believe that they provide useful insights about the accumulation patterns of cutaneous carotenoids. We remark that the advance of the current understanding about these processes is essential for the success of future biomedical initiatives in this area, notably those involving the noninvasive monitoring of the degree of photoprotection that cutaneous carotenoids can provide for individuals with distinct levels of constitutive pigmentation.

REFERENCES

[1] S. Piña-Oviedo, C. Ortiz-Hidalgo, and A.G. Ayala, "Human colors - the rainbow garden of pathology, What gives normal and pathologic tissues their color?," *Acta Pathol. Lab. Med.*, vol. 141, pp. 445–462, 2017.

[2] A.D. Lascari, "Carotenemia a review," *Nutrition*, vol. 20, no. 1, pp. 25–29, 1981.

[3] G. Tang and R.M. Russell, "Bioequivalence of provitamin A carotenoids," in *Carotenoids in Health and Disease*, N.I. Krinsky, S.T. Mayne, and H. Sies, Eds., pp. 279–294. Marcel Deck, New York, USA, 2004.

[4] S. Zerres and W. Stahl, "Carotenoids in human skin," *BBA - Molecular and Cell Biology of Lipids*, vol. 1865, pp. 158588:1–6, 2020.

[5] M.E. Darwin, W. Sterry, J. Lademann, and T. Vergou, "The role of carotenoids in human skin," *Molecules*, vol. 16, pp. 10491–10506, 2011.

[6] E. Edigin, I.R. Asemota, E. Olisa, and C. Nwaichi, "Carotenemia: A case report," *Cureus*, vol. 11, no. 7, pp. 1–4, 2019.

[7] S. Alaluf, U. Heinrich, W. Stahl, H. Tronnier, and S. Wiseman, "Dietary carotenoids contribute to normal human skin color and UV photosensitivity," *J. Nutr.*, vol. 132, no. 3, pp. 399–403, 2002.

[8] E. Hoerer, F. Dreyfuss, and M. Herzberg, "Carotenemia, skin colour and diabetes mellitus," *Acta Diabet. Lat.*, vol. 12, pp. 202–206, 1981.

[9] P.S. Bernstein and W. Gellermann, "Noninvasive assessment of carotenoids in the human eye and skin," in *Carotenoids in Health and Disease*, N.I. Krinsky, S.T. Mayne, and H. Sies, Eds., pp. 53–84. Marcel Deck, New York, USA, 2004.

[10] S.B.J. Pitts, L. Jahns, Q. Wu, N.E. Moran, R.A. Bell, K.P. Truesdale, and M.N. Laska, "A non-invasive assessment of skin carotenoid status through reflection spectroscopy is a feasible, reliable and potentially valid measure of fruit and vegetable consumption in a diverse community sample," *Public Health Nutr.*, vol. 21, no. 9, pp. 1664–1670, 2018.

[11] Y. Sharoni, W. Stahl, M. Danilenko, and J. Levy, "Noninvasive assessment of carotenoids in the human eye and skin," in *Carotenoids in Health and Disease*, N.I. Krinsky, S.T. Mayne, and H. Sies, Eds., pp. 165–196. Marcel Deck, New York, USA, 2004.

[12] S.R. Mohammed and S. Teelucksingh, "Not all that's yellow is jaundice," *J. Roy. Coll. Phys. Edin.*, vol. 52, no. 2, pp. 149–150, 2022.

[13] E.M. Zon, S.N. Khairudin, and S.H Haidar, "An orange baby: benign carotenemia in an infant," *IMJM*, vol. 22, no. 4, pp. 145–148, 2023.

[14] A.A. Fico, E. Petrela, E. Zajmi, N. Sinami, and D. Dobi, "Secondary carotenemia: Case report," *Med. Res. Chron.*, vol. 3, no. 2, pp. 203–205, 2016.

[15] F. Nakagami, Y. Nozato, K. Yamamoto, and H. Rakugi, "Carotenemia induced by iron deficiency," *BMJ Case Rep.*, vol. 14, pp. 1–2, 2021.

[16] K. Sawano and K. Nagasaki, "Carotenoderma with hypothyroidism," *Arch. Dis. Child*, vol. 107, pp. 615, 2022.

[17] R. Lee, M. M. Mathews-Roth, M. A. Pathak, and J. A. Parrish, "The detection of carotenoid pigments in human skin," *J. Investig. Dermatol.*, vol. 64, no. 3, pp. 175–177, 1975.

[18] H.D. Sesso and J.M. Gaziano, "Heart and vascular tissues," in *Carotenoids in Health and Disease*, N.I. Krinsky, S.T. Mayne, and H. Sies, Eds., pp. 473–490. Marcel Deck, New York, USA, 2004.

[19] D.I. Perrett, S.N. Talamas, P. Cairns, and A.J. Henderson, "Skin color cues to human health: carotenoids, aerobic fitness, and body fat," *Front. Physiol.*, vol. 11, pp. 392:1–14, 2020.

[20] S. Gupta, M.J. Bourke, and N.G. Burgess, "Pain and pigmentation: a puzzling presentation," *Gastroenterology*, vol. 160, pp. 1034–1036, 2021.

[21] S.L. Jacques, "Optical absorption of melanin," Tech. Rep., Oregon Medical Laser Center, 2001.

[22] S.A. Prahl, "Optical absorption of hemoglobin," Tech. Rep., Oregon Medical Laser Center, 1999.

[23] S.A. Prahl, "PhotochemCAD spectra by category," Tech. Rep., Oregon Medical Laser Center, 2001.

[24] T.F. Chen, G.V.G. Baranoski, B.W. Kimmel, and E. Miranda, "Hyperspectral modeling of skin appearance," *ACM Trans. Graph.*, vol. 34, no. 3, pp. 31:1–14, 2015, Supplemental video: https://www.youtube.com/watch?v=hKvIWS5H94s.

[25] G.V.G Baranoski, S.R. van Leeuwen, and T.F. Chen, "On the detection of peripheral cyanosis in individuals with distinct levels of cutaneous pigmentation," in *39th Annual International Conference of the IEEE Engineering in Medicine and Biology Society (EMBC)*, Jeju Island, South Korea, August 2017, pp. 4260–4264.

[26] M.J. Vrhel, R. Gershon, and L.S. Iwan, "Measurement and analysis of object reflectance spectra," *Color Research and Application*, vol. 19, no. 1, pp. 4–9, 1994.

[27] J.A. Jacquez, J. Huss, W. McKeehan, J.M. Dimitroff, and H.F. Kuppenhein, "Spectral reflectance of human skin in the region 235-700 mμ," *J. Appl. Physiol.*, vol. 8, pp. 212–214, 1955.

[28] S. Askew and G.V.G Baranoski, "On the dysfunctional hemoglobins and cyanosis connection: Practical implications for the clinical detection and differentiation of methemoglobinemia and sulfhemoglobinemia," *Biomed. Opt. Express*, vol. 9, no. 1, pp. 3284–3305, 2018.

[29] S.R. van Leeuwen and G.V.G Baranoski, "Elucidating the contribution of Rayleigh scattering to the bluish appearance of veins," *J. Biomed. Opt.*, vol. 23, no. 2, pp. 025001–1–17, 2018.

[30] T.F. Chen and G.V.G. Baranoski, "A physiologically-based framework for the simulation of skin tanning dynamics," in *Proc. of SPIE, Vol. 10877, Dynamics and Fluctuations in Biomedical Photonics XVI: Tissue and Cell Dynamics, SPIE Photonics West - BiOS*, M.J. Leahy V.V. Tuchin and R.W. Wang, Eds., San Francisco, CA, USA, March 2019, pp. 108770H–1–20, Supplemental video: https://www.youtube.com/watch?v=I1quYM34wWw.

[31] Natural Phenomena Simulation Group (NPSG), *Run HyLIoS (Melanoma Simulation) Online*, School of Computer Science, University of Waterloo, Ontario, Canada, 2022, http://www.npsg.uwaterloo.ca/models/hylios_ms.php.

[32] Natural Phenomena Simulation Group (NPSG), *Human Skin Data*, School of Computer Science, University of Waterloo, Ontario, Canada, 2014, http://www.npsg.uwaterloo.ca/data/skin.php.

[33] Y. Takita, M. Ichimiya, Y. Hamamoto, and M. Muto, "A case of carotenemia associated with ingestion of nutrient supplements," *J. Dermatol.*, vol. 2, pp. 132–134, 2006.

[34] R.W.G. Hunt, *Measuring Colour*, Ellis Horwood Limited, Chichester, England, 2nd edition, 1991.

[35] G.V.G. Baranoski and A. Krishnaswamy, *Light & Skin Interactions: Simulations for Computer Graphics Applications*, Morgan Kaufmann/Elsevier, Burlington, MA, USA, 2010.

[36] M. Stokes, M.D. Fairchild, and R.S. Berns, "Precision requirements for digital color reproduction," *ACM Trans. Graph.*, vol. 11, no. 4, pp. 406–422, 1992.

[37] D.H. Brainard, "Color appearance and color difference specification," *The Science of Color*, vol. 2, pp. 191–216, 2003.

[38] M. Mahy, L. Van Eycken, and A. Oosterlinck, "Evaluation of uniform color spaces developed after the adoption of CIELAB and CIELUV," *Color Research and Application*, vol. 19, no. 2, pp. 105–121, 1994.